Braz J Phys (2013) 43:268–280
DOI 10.1007/s13538-013-0149-7

Physics and Its Interfaces with Medicinal Chemistry and Drug Design

Ricardo N. Santos · Adriano D. Andricopulo

Received: 22 May 2013 / Published online: 9 July 2013

Abstract Medicinal chemistry is a multidisciplinary subject that integrates knowledge from a variety of fields of science, including, but not limited to, chemistry, biology, and physics. The area of drug design involves the cooperative work of scientists with a diverse range of backgrounds and technical skills, trying to tackle complex problems using an integration of approaches and methods. One important contribution to this field comes from physics through studies that attempt to identify and quantify the molecular interactions between small molecules (drugs) and biological targets (receptors), such as the forces that govern the interactions, the thermodynamics of the drug–receptor interactions, and so on. In this context, the interfaces of physics, medicinal chemistry, and drug design are of vital importance for the development of drugs that not only have the right chemistry but also the right intermolecular properties to interact at the macromolecular level, providing useful information about the principles and molecular mechanisms underlying the therapeutic action of drugs. This article highlights some of the most important connections between physics and medicinal chemistry in the design of new drugs.

Keywords Medicinal chemistry · Physics · Drug design · Molecular interactions

1 Introduction

Over the last century, the development of safe and effective drugs has contributed for improving the quality of life and increasing life expectancy of children, adults, and the elderly worldwide. According to the World Health Organization, life expectancy at birth globally was 68 years, in 2009, ranging from 57 to 80 years in low- and high-income countries, respectively [1]. For use in humans, a drug should have a good balance between pharmacodynamics (defined as the study of the biological and physiological effects resulting from the interactions between drugs and biological systems) and pharmacokinetics (defined as the study of the time course of the drug concentration in different fluids of the body, incorporating absorption, distribution, metabolism, and excretion properties), as well as safety [2–4]. Basically, a drug has to be absorbed to get into the blood circulation and to diffuse to various tissues and organs in the body, without undergoing substantial biochemical modification or degradation (metabolism), to finally bind to a specific macromolecule (target protein) and exert the desired therapeutic action [5].

For the past decades, scientists have been gaining increasing control over critical processes in drug design, evaluating (i.e., measuring, predicting, inferring, and understanding) physicochemical properties in order to ensure optimal pharmacodynamics and pharmacokinetics, and consequently, developing better drugs for a variety of human diseases. Drug design is a multidisciplinary research field covering several aspects of chemistry and biology together with strong and fruitful interfaces with physics. Innovative strategies, methods, and tools have benefited from several scientific and technological advances to give scientists an exceptional understanding of the basic principles and mechanisms underlying the processes of protein–ligand binding and biological activity [6–8]. This is an area where physics makes one of the most substantial impacts in drug design, by reducing the complexity of chemical and biological systems to a collection of more simple elements and trying to describe it with models ruled by fundamental theories. In this respect, tremendous scientific progress has been achieved in the description of molecular interactions, improving our understanding of their role in medicinal chemistry and drug design. This article covers some of the most important connections between physics and medicinal chemistry in the

Electronic supplementary material The online version of this article (doi:10.1007/s13538-013-0149-7) contains supplementary material, which is available to authorized users.

R. N. Santos · A. D. Andricopulo (✉)
Instituto de Física de São Carlos, Universidade de São Paulo, 13560-970 São Carlos, São Paulo, Brazil
e-mail: aandrico@ifsc.usp.br

design of new drugs. Three short videos were produced especially for this article with the goal of ensuring a more comprehensive and insightful understanding of the molecular systems here described.

2 Complex Systems and Drug Design

Biological systems stand at the pinnacle of natural complexity, expressed as the most instigating set of phenomena called life. For instance, proteins are complex functional and dynamic structures whose interfaces with the surrounding fluids govern their interactions with small-molecule ligands. Knowing the three-dimensional structure of a target protein is extremely important, but at the same time it is only the beginning of a long journey in drug discovery [9]. One of the main challenges is to understand the functional and physicochemical properties of these complex systems and how they are affected by a disease or dysfunction, as well as by the action of a drug. The use of physical models along with computational methods to describe these systems has generated several remarkable scientific contributions, which have helped the development of drugs with novel action mechanisms [10, 11].

In a practical sense, investigations of biological systems through physical models face the challenge of dealing with a vast number of elements, even in the simplest living cells. As an example, let us try to estimate the number of molecules in a human cell from very basic data. As a first step, it can be assumed that an average mammalian cell has approximately a volume of 4×10^{-9} cm^3, 70 % of which are occupied with water. The cell can approximately be regarded as full of water for the stated purpose [12]. Given that 1 m^3 of water weighs almost 1,000 kg at 37 °C and, therefore, contains nearly 3.3×10^{28} water molecules (using Avogadro's constant and the water molar mass), when the ratio is multiplied by the cell volume, it results that one human cell has approximately 1.3×10^{14} atoms. The classical-mechanics simulation of a physical model for a cell with this large number of atoms is computationally unfeasible, even with today's most powerful machines. The situation becomes worse when considering the many different molecular components besides water that exist in a real cell. Furthermore, the study of several phenomena at this level would require quantum chemistry. This seemingly unsolvable problem can nonetheless be faced by breaking down the system into a series of smaller, more treatable problems.

3 A Practical Example in Anticancer Drug Discovery: The Binding of Taxol to β-Tubulin

One critical step in drug design is the selection of a macromolecular target, usually a protein involved in the process of a specific disease [13]. Proteins are biological macromolecules built from the assembly of small molecules called amino acids (i.e., organic compounds having amine and carboxylic acid functional groups attached to an α-carbon atom, along with a side-chain specific to each amino acid type) through peptide chains in a specific sequence that dictates their shapes and functions, as shown in the animation (Electronic Supplementary Material (ESM) 1) [14]. Proteins perform a vast number of functions in cells, ranging from the maintenance of scaffolds and cellular division to the catalysis of chemical reactions. As cell metabolism is carried out by exquisite and dynamic machinery in perfect synchronization, the modulation of the activity of a particular protein in a biochemical pathway could lead to drastic biological responses, such as the manifestation of a disease or disorder in humans [15]. Accordingly, most drugs bind to and modulate the biological responses of specific target proteins to promote their therapeutic action.

Cancer is a large group of diseases that can affect any part of the body. One defining feature of cancer is the rapid creation of abnormal cells (tumors) that grow beyond their usual boundaries, and which can then invade adjoining parts of the body and spread to other organs, in a process referred to as metastasis [16, 17]. Cancer is a leading cause of death worldwide, accounting for 7.6 million deaths (around 13 % of all deaths) in 2008 [1]. Lung, stomach, liver, colon, and breast cancers cause most cancer deaths each year. The American Cancer Society estimates that cancer will cause over 1.6 million deaths in the USA during 2013 [18].

The process of growth and division of cells is usually accompanied by intense polymerization of microtubules, which act physically by separating two cells and their components after division and providing frameworks for cellular transport and shape. In tumor cells, the uncontrolled and rapid growth is sustained by an intense activity of polymerization and depolymerization of microtubules. The anticancer drug paclitaxel (Taxol®, a registered trademark of Bristol-Myers Squibb Company), which is extracted from the bark of Pacific Yew, has the ability to interact with microtubules promoting its stabilization, as shown in the animation (ESM 2) [19–23]. As the activity of this protein is much more intense in cells that are in constant division, the effect of Taxol in tumor cells is similarly more pronounced when compared with its effect in normal cells—hair follicle cells are exceptions, because they grow and divide very rapidly [24, 25]. As a practical example, the protein tubulin was chosen to characterize a complex biological system of great importance in the design of novel anticancer agents, with emphasis to the Taxol binding site in the β-tubulin pocket of the αβ-tubulin heterodimer. This example will be used repeatedly throughout this paper.

4 Molecular Docking and the Problem of Conformational Search

After the identification of a target protein related to a disease, one of the key steps in drug discovery is the selection of promising molecules that are able to interact with the target receptor to produce the desired pharmacological action. The study of the binding mode of these molecules is useful to guide the design of novel compounds with improved properties.

A valuable approach to identify molecules that bind to specific receptors comprises the prediction of their binding affinity through physical models applied to computational simulation methods. *Molecular docking* is one of the most widely used methods to predict the binding mode of a ligand into the binding pocket of a receptor (see Fig. 1) [26–28]. Energy minimizations of the unbound and bound structures are carried out to maximize inter- and intramolecular interactions and to identify the binding mode that is more likely to occur in a real system.

The molecular docking procedure can be used to predict the binding profile of large ligand databases (typically in the range of thousands to millions, including compounds from natural and synthetic sources), as a tool to select the most promising candidates for experimental evaluation. This high throughput in silico (i.e., *computer based*) screening procedure is called *virtual screening* [29–31].

The ability of the computational models to predict binding affinities entails an accurate description of the main molecular features of protein–ligand complexes, including the conformational changes involved in the molecular recognition process. Bearing in mind that the atoms from each of the considered molecules are linked by covalent bonds, it is possible to restrict the definition of conformation as the spatial arrangement of atoms adopted with the rotation of all single-bond angles (Fig. 2) [32].

The identification of the most plausible conformation for a complex involves the systematic assessment of the conformational space in a process known as *conformational search*. This can be a very challenging puzzle even for a simple small molecule, since the number of possible conformations increases drastically with the number of rotatable bonds (a phenomenon commonly called *combinatorial explosion*) [32]. A general expression for the number of possible conformations of a molecule with N rotatable bonds can be given as follows:

$$\textit{Number of conformations} = \prod_{i=1}^{N} \frac{360}{\theta_i}, \tag{1}$$

where θ_i is the torsional increment chosen for bond i during the conformational search.

The huge number of possible conformations for a small protein molecule can illustrate the unwelcome phenomenon of combinatorial explosion. The sequence of amino acids (polypeptide chain) is unique and specific to a given protein. The association of amino acids in protein synthesis (ESM 1) occurs through a condensation reaction involving the carboxyl group of an amino acid and the amino group of another amino acid. In the polypeptide chain, each amino acid contributes with three bonds for the protein backbone chain (nitrogen to α-carbon, α-carbon to carbonyl carbon, and carbonyl carbon to nitrogen, as shown in Fig. 3). Because of the partial double character of the bond formed by the carbonyl carbon and nitrogen, resonance effects restrict the peptide bond to a planar form. Therefore, the only bonds allowed to rotate freely in the protein main chain are those between carbons (assigned as ψ in Fig. 3), and between the nitrogen and the α-carbon of the condensed amino acid (assigned as φ in Fig. 3) [14]. When considering only these two rotatable bonds of the main chain in a protein, and ignoring the rotatable bonds of the specific side-chains, it is possible to estimate the number of conformations for a hypothetic system. This can be further simplified if only few angles of rotation fit to local minima and are adopted by the protein. Insulin, one of the smallest proteins in the body, is composed of 51 amino acids. For example, taking into account that the number of rotatable bonds (φ and ψ) in the main chain is 100 (Fig. 3) and only three rotational angles are energetically possible for each bond (θ_i=120° for all bonds), 3^{100} (approximately 5.2×10^{47}) conformations will be generated.

The conformation of proteins can be experimentally determined by X-ray crystallography or nuclear magnetic resonance spectroscopy. In these cases, the solved models represent the average (most representative) conformations assumed

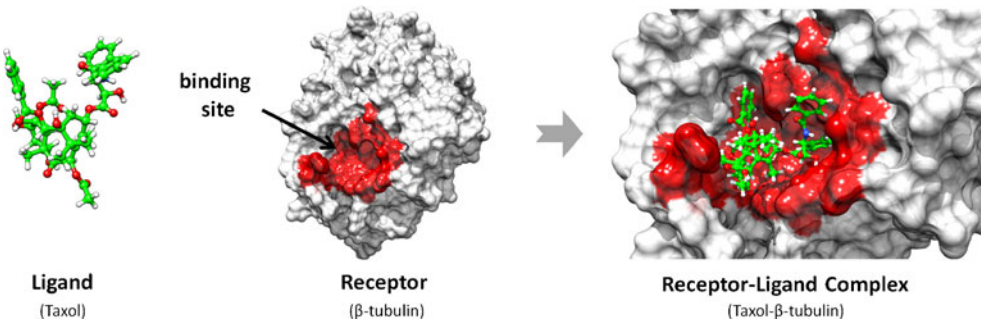

Fig. 1 Interaction of Taxol in the β-tubulin binding site to form a receptor–ligand complex. The prediction of the binding conformation and energy of the ligand in its binding site is the main goal of the molecular docking strategies (colored online)

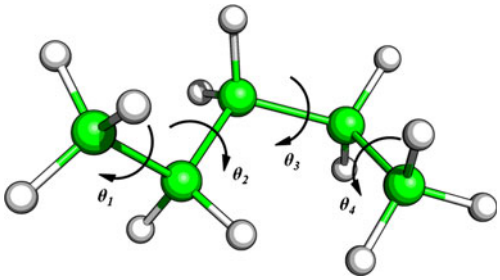

Fig. 2 Internal degrees of freedom that define the conformation of the pentane molecule by the rotation of angles θ of bonds (θ_1–θ_4). Carbon and hydrogen atoms are shown as *green* and *white*, respectively (colored online)

by the molecules in solution. The structural data are stored in the *Protein Data Bank* (PDB) and freely available to the worldwide scientific community [33]. The 3D-structures solved by experimental methods represent the unbound (*apo*, ligand-free) conformation of the protein or its structure in complex with a ligand (*holo*, ligand-bound). The goal of docking methods is to determine the conformational changes in the target and ligand structures caused by their mutual interaction to form a binary complex. Considering a non-allosteric target protein, the conformational changes far from the binding site for the formation of complexes are negligible and the conformational search can be restricted to the binding site region, incorporating the ligand and the side chains of the surrounding residues.

Conformational search methods can be classified broadly into three types: (1) systematic, (2) stochastic, and (3) molecular dynamics simulations [11, 26, 32, 34–36]. Systematic search methods (1) try to explore all conformational space using rational methodologies to face the problem of combinatorial explosion. A commonly utilized systematic search method is the *incremental construction*. In this approach, the ligands are broken down into smaller fragments that are classified and used to identify regions of optimal interaction in the receptor binding site (Fig. 4). Starting from an initial docked fragment (called *seed*), the ligand is built through the

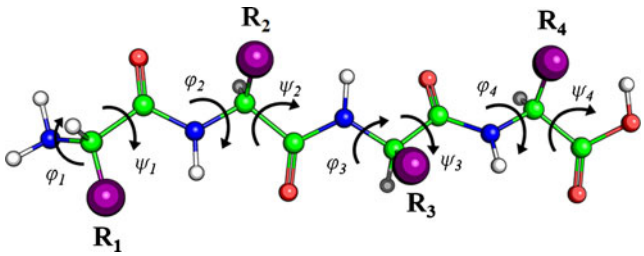

Fig. 3 Internal degrees of freedom of the backbone of a protein chain. The number of rotational bonds drastically increases the number of possible conformations leading to the problem of combinatorial explosion. Oxygen, nitrogen, carbon, and hydrogen atoms are depicted in *red*, *blue*, *green*, and *white*, respectively. *Purple spheres* (R) represent the side chains that differ for each amino acid type (colored online)

association of the remaining fragments and the interactions are optimized in each step. Finally, all conformations obtained from distinct initial fragments are classified and evaluated by scoring functions.

Stochastic methods (2) randomly change the conformation parameters of a system, generating different conformation populations. A powerful approach is the application of genetic algorithms. In this case, each ligand or residue is represented by a vector containing all parameters necessary to describe its conformation (e.g., rotational angles, represented in Fig. 2, together with coordinates and orientation of its center of mass), and these parameters are randomly modified to generate a diverse population of possible conformations. The propagation of each individual in this population is based in the Darwin's natural selection principle, which states that only the best adapted individual survives along a long process of population selection cycles. In this case, the level of adaption should be proportional to the binding energy related to the complex formation. Therefore, after each cycle only a fraction of the population, corresponding to the most adapted samples (evaluated by scoring), is kept and used to generate another population by random modifications of their parameters.

Molecular dynamics is a computational method used to simulate interactions between ligands and receptors along time using a deterministic approach that numerically solves Newton´s equation of motion for the system and use these results to calculate the positions and velocities of all particles after short time intervals. This process is repeated iteratively by calculating and solving the equation of motion in a way that the movement of each particle in the system can be integrated along time. The initial velocities of the system are randomly attributed to all particles obeying a Boltzmann distribution that agrees with the specific temperature of the real system. This method has the advantage of explicitly consider the effects of solvent and temperature during the process of complex formation. Nevertheless, the high computational time required to complete the procedure makes this approach less attractive and practical for *virtual screening* studies, which involve the simulation of huge systems and the evaluation of large databases of molecules. Moreover, molecular dynamics simulations are usually unable to overtake the high-energy barriers necessary to a system assume a different conformation within a reasonable computational time. The statistical evaluation of the problem involves an ensemble of molecular simulations instead of a single observation, which drastically increases the computational time required to run the analysis [26, 32]. Despite these limitations, there has been substantial progress with the advances in computational power and the development of new simulation methodologies, allowing the application of molecular dynamics in an ever-increasing number of tasks in medicinal chemistry and drug design.

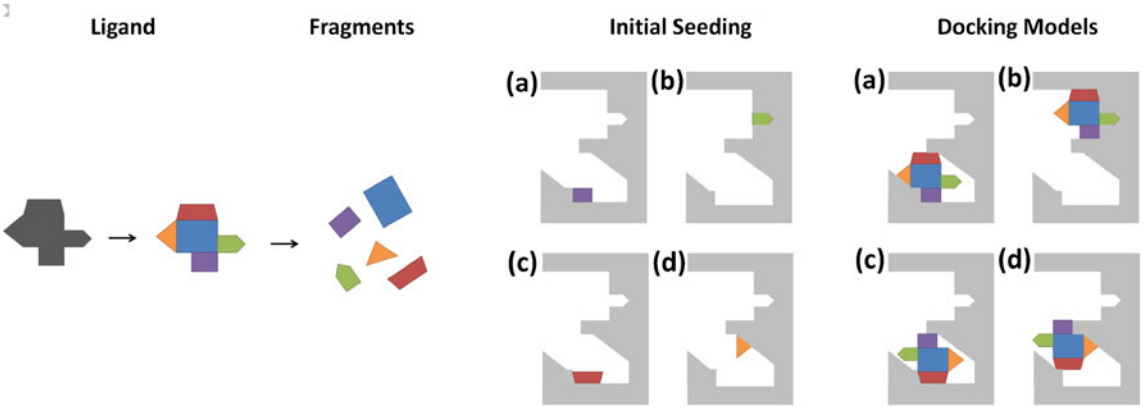

Fig. 4 The incremental construction method is used to explore the conformational space into the receptor pocket in order to identify potential ligand binding conformations. After shredding a ligand structure in several fragments (*colored blocks*), the next step involves the identification of complementary regions in the receptor binding site. The initial docked fragments are grown by iterative integration and minimization of the entire ligand. This process leads to a diversity of binding complexes that are further evaluated to provide a suitable solution (colored online)

5 Drug Binding

The well-known class of enzyme inhibitors represents about 50 % of the drugs in clinical use. These compounds act by binding to and inhibiting the activity of specific enzymes, in a process that usually results in the restoration of the body's normal metabolism. The best-selling drug in the history of the pharmaceutical industry, the cholesterol-lowering atorvastatin (marketed by Pfizer under the trade name Lipitor®, Fig. 5a), is a good example of successful enzyme inhibitor. This drug competitively binds to the site of the natural substrate, HMG-CoA (3-hydroxy-3-methylglutaryl CoA), of the enzyme HMG-CoA reductase (Fig. 5b), blocking the formation of mevalonate, an important precursor of cholesterol biosynthesis [37].

For a better understanding of the binding process, the inhibitory activity of atorvastatin (as in the case of many other drugs) can be represented by a simple system consisting of the ligand (atorvastatin) and the receptor (HMG-CoA reductase). Ligand binding can be regarded as the process of interaction by physical contact resulting in attractive forces between a small-molecule ligand and a macromolecule receptor during a period of time [38, 39]. The equilibrium between receptor (**R**), ligand (**L**) and the receptor–ligand complex (**R**–**L**) in solution can be represented as follows:

$$R + L \underset{K_d}{\overset{K_a}{\rightleftharpoons}} R\text{-}L \tag{2}$$

The rates of complex association and dissociation are given by K_a and K_d constants, respectively. The complex dissociation constant K_d can be used to express the binding affinity of a ligand (**L**) to a receptor (**R**) and is usually defined as a binding constant:

$$K_d = \frac{[R][L]}{[R\text{–}L]}. \tag{3}$$

In this case, the magnitude of K_d is proportional to the probability of the complex to dissociate (i.e., the magnitude of K_d is inversely related to the strength of the complex), and

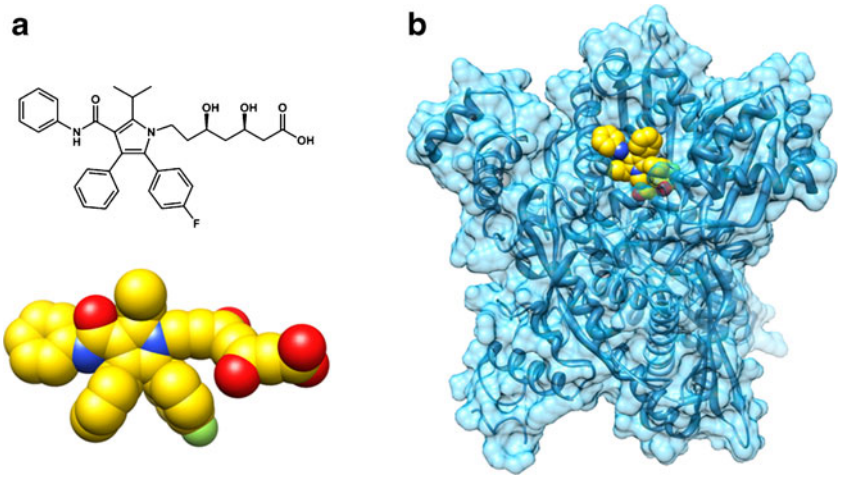

Fig. 5 **a** Chemical structure representation of atorvastatin. **b** Crystallographic structure of atorvastatin in complex with HMG-CoA reductase (PDB ID, 1HWK; colored online)

is expressed in moles per liter (or molarity (M)). The free energy due to changes in a system can be represented by changes in enthalpy and entropy using a fundamental thermodynamics relationship:

$$\Delta G = \Delta H - T\Delta S, \tag{4}$$

where ΔG is the difference in free energy (also called Gibbs free energy) between the energy of the final and the initial configuration of a system, and ΔH and ΔS are the changes in enthalpy and entropy, respectively. T corresponds to the temperature (in Kelvin) of the system. Another useful relationship that can be derived from thermodynamics relates the dissociation equilibrium constant (Eq. 3) to the change in energy of the system (Eq. 4). A detailed discussion of this expression can be found elsewhere [40].

$$\Delta G = \Delta G^{\circ} - RTln\frac{K_d}{C^{\circ}}, \tag{5}$$

where ΔG° is the free energy change for a reaction performed under standard conditions (pressure=1 atm, T=298 K, and concentration=1 M for components in solution), C° is the standard state concentration and R is the gas constant (in joules per Kelvin per mole). When a reaction is at equilibrium, the change in free energy (ΔG) is zero and ΔG° stands for the free energy of binding ($\Delta G^{\text{binding}}$). Therefore, Eq. (5) can be simplified as follows:

$$\Delta G^{binding} = RTln\frac{K_d}{C^{\circ}}. \tag{6}$$

The choice of the Gibbs free energy to describe the energy of binding is suitable because biochemical and biological studies are commonly conducted under constant pressure. It can also be shown that the exact change in free energy as a result of a transition between two states of a system (A and B, for example, for unbound molecules to form a bound complex) can be calculated considering the Hamiltonians of each configuration [41–43]:

$$\Delta G = G_B - G_A = -RTln\langle e^{-(H_B - H_A)/RT}\rangle_A , \tag{7}$$

where G_A and G_B are the free energies of configurations A and B of the system, and H_A and H_B are the Hamiltonian describing these states. Brackets $\langle\ \rangle_A$ mean that the average of a thermodynamic ensemble for state A was evaluated. Equation (7) states that the exact configurations assumed by a system during a transition process (as the formation of a complex by noncovalent interactions between two molecules) are known and it is possible to calculate the associated free-energy change, as well as to predict the binding affinity of the ligand.

As the computational processing power is insufficient to represent an adequate ensemble and to describe systems of ligands and receptors in solution, a reasonable approach is to estimate the free energy of binding considering only the contributions of the bound and unbound conformations. This approximation is known as the *end-point* free energy method [43].

6 Prediction of Receptor–Ligand Interactions by Physical Models

After a ligand binding conformation model is achieved, the next step involves the use of molecular docking approaches to evaluate the energy and the plausibility of this conformation. This task can be completed by the calculation of the energies associated to each state. As the systems studied by molecular modeling are too large to be faced by quantum mechanical methods (even those that consider only valence electrons), the procedures employed to evaluate the energy of a system conformation usually apply force fields based on classical molecular mechanics [32, 36, 39]. The success of this approach in providing good predictive results is only possible thanks to the Born–Oppenheimer approximation. This principle states that the high ratio between the mass of atoms and electrons (a factor of 1:1,836) in a molecule allows separation of the nuclear and electronic motions, and parametrization of the system energy as a function of the nuclear coordinates. In quantum mechanics, as shown in Eq. (8), this means that the total wave function of a molecule (Ψ_{total}) can be broken into its nuclear and electronic components (Ψ_{nuclear} and $\Psi_{\text{electronic}}$) and these wave functions can be solved separately [32, 44]:

$$\psi_{total}\left(\vec{r_i},\vec{R}_j\right) = \psi_{electronic}\left(\vec{r_i},\vec{R}_j\right)\psi_{nuclear}\left(\vec{R}_j\right), \tag{8}$$

where $\vec{r_i}$ and $\vec{R}_j$ are the electron and nuclear coordinates of all particles in the system.

The energy variation attributable to conformational changes can be calculated by considering inter- and intramolecular contributions and applying force fields using the atomic coordinates of the system. The energy variation in the binding process can be represented as a sum of energy contributions related to different phenomena occuring during molecular association [32, 36, 39]:

$$\Delta G_{bind} = \Delta G_{solvent} + \Delta G_{conformation} + \Delta G_{intermolecular} + \Delta G_{motion}. \tag{9}$$

In this equation, $\Delta G_{\text{solvent}}$ represents the energy contribution attributable to the disruption and formation of interactions between the solvent, ligand, protein and binding complex. $\Delta G_{\text{conformation}}$ accounts for conformational changes in the protein and ligand, and $\Delta G_{\text{intermolecular}}$ is the energy originated during the binding process from interactions between ligand and protein. The term ΔG_{motion} has an entropic nature and comprises the change in entropy due to the loss of degrees of

freedom associated with freezing internal rotations of the protein and the ligand, and the change in translational, rotational, and vibrational free energies caused by the formation of the complex. Potential energy changes (corresponding to the first three terms on the right-hand side of Eq. 9) can be evaluated with simple force fields containing terms related to the forces defined by the atomic coordinates of the system. A general force field to calculate the potential energy $V_{(r^N)}$ in a system containing N atoms with coordinates specified by a position vector r is given by the following expression:

$$V_{(r^N)} = \sum_{i=1}^{N}\sum_{j=i+1}^{N}\frac{q_i q_j}{4\pi\varepsilon_{ij} r_{ij}} + \sum_{i=1}^{N}\sum_{j=i+1}^{N} 4E_{ij}\left[\left(\frac{\sigma_{ij}}{r_{ij}}\right)^{12} - \left(\frac{\sigma_{ij}}{r_{ij}}\right)^{6}\right] \sum_{bonds}\frac{k_i}{2}\left(l_i - l_{i,0}\right)^2 + \sum_{angles}\frac{\chi_i}{2}\left(\theta_i - \theta_{i,0}\right)^2 + \sum_{torsions}\frac{Vn}{2}\left(1+\cos(n\omega-\gamma)\right) \quad (10)$$

The first two terms on the right-hand side of Eq. (10) denote the contributions from non-bonding Coulombic and van der Waals interactions, respectively. These forces should be calculated for every atom pair in the system, considering also different molecules. In these terms, q_i and q_j represent the partial charges of the atom pair used for calculation; ε_{ij} is the dieletric constants in vacuo and between atoms i and j; r_{ij} is the distance between the atoms; and σ_{ij} is the van der Waals collision diameter for atom pairs.

The Coulomb interactions in the first term on the right-hand side of Eq. (10) result from the different atomic charges in a molecular system. Among these are interactions between complementary charged groups, permanent dipoles and charged groups and between permanent dipoles (Fig. 6). The strongest interactions are between charged groups (also known as electrostatic or ion–ion interactions, Fig. 6a). They occur between groups with opposite charges and their magnitude is inversely proportional to the distance between these charged groups. Differences of electronegativity of atoms in a molecule result in permanent dipoles that can interact with charged groups (ion–dipole interactions, Fig. 6b) or with other dipoles (dipole–dipole interactions, Fig. 6c). Ion-dipole and dipole–dipole interactions fall with the square and cube of distance, respectively, and become weaker faster than ion-ion interactions as the separation grows.

The hydrogen bond is an exceptionally important interaction in biological systems, which occurs between an electron-rich heteroatom with a lone pair of electrons (usually nitrogen and oxygen) and an electron-deficient hydrogen [45, 46]. In this interaction, the orbital of the lone pair of electrons in the electron-rich atom interacts and overlaps with the atomic orbital of the electron-deficient hydrogen, generating an attraction force stronger than an ordinary dipole–dipole interaction (Fig. 7). The strength of hydrogen bonds varies with the relative orientation and distance of dipoles. Optimal hydrogen-bond interaction is achieved when the angle between the dipoles is 180°, and the distance between the hydrogen and the electron-rich atom (hydrogen bond acceptor) falls in the range of 1.5–2.2 Å [45]. Hydrogen bonding is one of the most important intermolecular forces for protein–ligand complex formation.

In docking Coulomb-interaction calculations, the partial charges of the atoms in the system are usually calculated using rapid calculation procedures, such as the Gasteiger and Marsilli method, or with more accurate, computationally intensive processes, such as the CHELPG calculation. Additional details on these methods can be found elsewhere [32, 47]. The second term in Eq. (10) accounts for hydrophobic (also called van der Waals) interactions. The Lennard-Jones potential describes this interaction, whose behavior is shown in Fig. 8.

The importance of van der Waals potential becomes more significant for very short distances, presenting a balance between attractive and repulsive potentials (the r^{-6} and r^{-12} terms on the right-hand side of Eq. (10), respectively). The predominant attractive contribution for long-range distances is due to dispersive forces (also called *London forces*) caused by the interaction of electron clouds of atoms with similar electron distributions. The fluctuations of an electron cloud can generate an instantaneous dipole for an atom, which can in turn induce other aligned dipoles in nearby atoms. This effect generates the

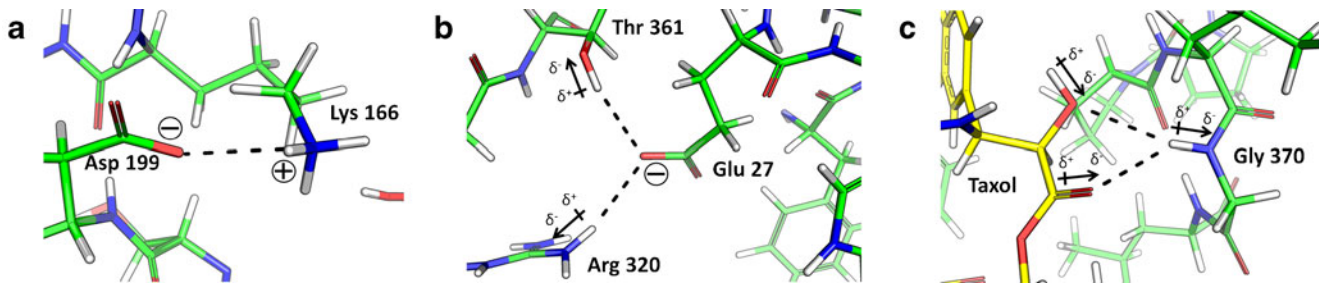

Fig. 6 Examples of Coulomb interactions employing the crystallographic structure of β-tubulin bound to Taxol (PDB ID, 1JFF). Carbon, oxygen, nitrogen, and hydrogen atoms are depicted in *green* (*yellow* for Taxol), *red*, *blue*, and *white*, respectively. **a** Ion–ion interactions between a negatively charged residue aspartate (Asp 199) and a positively charged residue lysine (Lys 166). **b** Ion–dipole interactions between a negatively charged residue glutamate (Glu 27) and the partially positive regions of two dipoles present in arginine and threonine residues (Arg 320 and Thr 361, respectively). **c** Dipole–dipole interactions between the partially positive region of a dipole of glycine residue (Gly 370) and the partially negative regions of dipoles of Taxol. These interactions contribute to the high binding affinity of Taxol to β-tubulin (colored online)

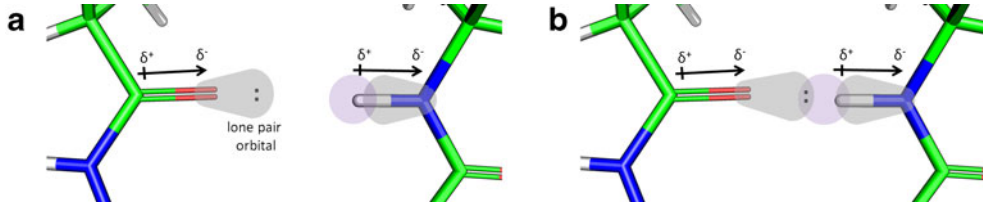

Fig. 7 Illustration of the hydrogen-bonding interaction between an electron-rich oxygen atom (with a lone pair of electrons, colored in *red*) and an electron-deficient hydrogen (colored in *white*, attached to a nitrogen atom, colored in *blue*). As the nitrogen has a greater electronegativity than hydrogen, the deformation of the electron cloud towards nitrogen results in a partially positive charge for hydrogen. The orbital containing the lone pair can superpose the orbitals participating in the hydrogen covalent bond generating a weak sigma bond that is called *hydrogen bond*. As the electron-rich atom (oxygen) partially receives the hydrogen atom, it is usually called *hydrogen bond acceptor*. The electron-rich atom (nitrogen, covalently bonded to hydrogen) that shares its hydrogen is called *hydrogen bond donor* (colored online)

attractive inductive force of van der Waals interactions [32, 48]. When these two atoms are brought together, the potential reaches an optimal minimum hydrophobic interaction (r_m distance in Fig. 8) supported by dispersive forces with maximum energy E. As the atoms get closer, the repulsive contribution increases and quickly overcomes the attractive contribution for distances smaller than the collision diameter σ. This is caused by the overlapping electron clouds and the repulsion between same-spin electrons. The short-range repulsions are also known as *exchange forces* and can be explained by the Pauli principle, which states that two electrons in a system cannot have the same set of quantum numbers.

The Coulomb and van der Waals contributions to Eq. (10) reflect the complementarity between the interacting molecules in the system. For a ligand to bind to a receptor, it must be close to the protein surface at a particular binding site and have highly specific molecular features (steric, electrostatic, and hydrophobic complementarity), much in the same way that a key must fit a lock. This leads to a high level of binding affinity, resulting in lower K_d values. Figure 9 shows the partial charges calculated for Taxol bound to β-tubulin by the Gaisteiger and Marsili method [49]. As can be seen, during the binding process the conformations assumed by the ligand and the amino acid residues in the binding site are arranged to maximize the electrostatic interactions between the opposite partial charges, resulting in optimum alignment between the system dipoles. This orientation of dipoles is an essential step for the formation of protein-ligand complexes.

The remaining terms in Eq. (10) account for the internal energy changes associated with conformational modifications attributable to bond torsions, stretching and bending, respectively (Fig. 10). These internal changes also play a significant role in the receptor–ligand binding strength. When the conformational energy of a molecule in its bound state and in solution (unbound) is very similar, there is no energy cost involved in conformational changes and the enthalpy of binding is simply the difference between broken and formed interactions during the formation of the complex. In the cases where the bound state adopts a higher-energy conformation, the energy involved in the process of binding must be compensated by other gains in energy during complex formation. This could lead to an apparent lower binding affinity between ligand and protein.

The simplest method, one that is nonetheless effective, to estimate the energy changes due to bond stretching to a distance l is to regard the bonds between atoms as springs (Fig. 11a), and to apply Hooke's law to them (third term on the right-hand side of Eq. 10). In this case, the energy increases with the square of the bond displacement from its natural length (l_0), and the strength of different bonds can be expressed by a spring-force constant k. The harmonic potential resulting from Hooke's law does not correspond to a real bond-stretching potential (Fig. 11b), although it provides a good approximation to describe events near the minimum bond energy. As the forces between covalently bonded atoms are strong, a high amount of energy is necessary to substantially stretch a covalent bond length between two atoms. Therefore, the Hooke's potential is suitable to describe small bond length deviations caused by intermolecular interactions, which frequently occur in the association of molecules [32].

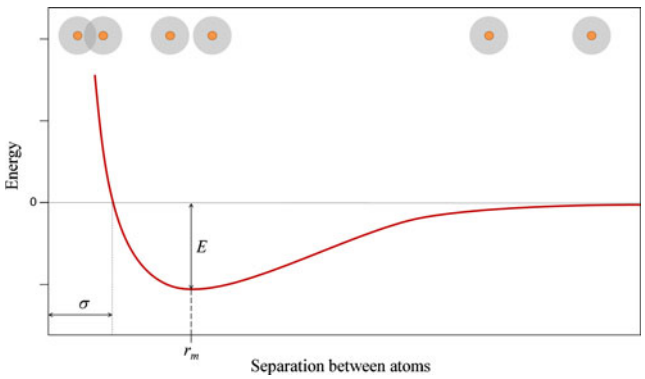

Fig. 8 Lennard–Jones potential for van der Waals interactions between two identical atoms. A representation of potential energy changes (Lennard–Jones potential, *red line*) according to the approach of two atoms (nuclei represented by *small orange spheres*) and superposition of their electron clouds (spheres colored in *gray*) is depicted above. The constant r_m represents the separation between atoms minimizing energy and maximizing the van der Waals interaction, σ is the collision diameter at which energy is zero, and E is the potential minimum (also called well depth; colored online)

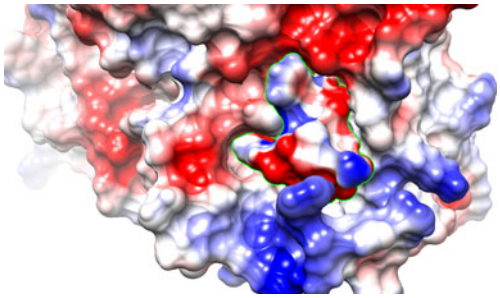

Fig. 9 Partial charge distribution for the atoms of the complex formed by Taxol and β-tubulin. Partially positively and negatively charged regions are colored in *blue* and *red*, respectively. Hydrophobic regions for the van der Waals contacts are depicted in *white*. In this molecular representation, the small-molecule ligand is represented by the *green contour* (colored online)

Similarly to the bond-stretching term, the angle bending (fourth term on the right-hand side of Eq. 10) energies can be well described by Hooke's law considering the displacement of the bond angle (θ) from its natural position (θ_0). The energy involved in this process is also weighted by a force constant χ. The energies associated with this displacement are considerably high since they are related to the resulting geometry of the molecules and the optimal orientation of the orbitals involved in bonding formation [32].

The last term in Eq. (10) is associated to the energy changes by rotations around single bonds. By varying the angle of a bond by rotation from 0° to 360°, the molecular groups on each side of the bond get closer and move away periodically, accordingly to the number and volume of groups bound to the atoms of the rotated bond. The energy oscillation can be described by a periodic function that considers every possible angle ω of torsion, as in the last term of Eq. (10). The number of minimum points in the potential function for complete rotation is represented by the multiplicity constant n in Eq. (10). The barrier necessary for a dihedral to switch from different minimum points is represented by the potential barrier V_n. Figure 12 illustrates the torsional potentials for different V_n, n, and γ.

The energy contributions here discussed, presented in Eq. (10), account for the enthalpy part of the Gibbs free-energy changes (Eq. 4). To achieve a sufficiently accurate

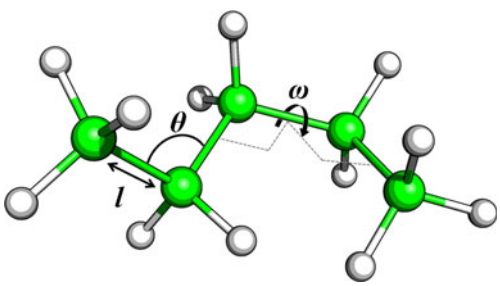

Fig. 10 Bonded terms considered in the calculation of conformational energies changes of a molecule (colored online)

Gibbs free energy for the binding process, major entropic effects must be considered. The association of two molecules to form a receptor–ligand complex freezes the translational and rotational degrees of freedom and, consequently, lower both the entropy and binding strength. Another source of entropy change is the redistribution of solvent molecules during the binding. When free in solution, the receptor and ligand are surrounded by water molecules that have to be displaced from the organized layer they form around the molecules to allow molecular interaction and binding to form a complex (Fig. 13). In addition, water molecules that are surrounded by nonpolar regions of a molecule can only interact between them and form well-ordered solvation layers. The release of these water molecules into the bulk solvent raises the entropy and makes an important contribution to the binding affinity [11, 32, 39].

Other correction terms can be added to Eq. (10) in order to improve the accuracy of energy calculations. Terms representing energy changes owing to dihedral torsions, solvation, freezing of rotational and translational degrees of freedom, as well as specific terms such as hydrogen-bond potentials, are often used to improve the accuracy of complex-conformation prediction. On the negative side, the inclusion of these correction terms can substantially increase the computational time.

7 Measuring Drug Binding Energies

After new ligands are identified from large libraries of compounds, the ability to bind to the target receptor has to be confirmed experimentally, in the hope to find overall good correspondence between experimental (in vitro) and predicted (in silico) affinities. Isothermal titration calorimetry (ITC) is one of the most common and useful methods for quantitative data collection to evaluate ligand binding and the corresponding energies. In a typical ITC experiment, the ligand of interest (**L**) is introduced in a calorimeter containing a solution of the target receptor with known concentration. Once the ligand binds to a receptor to form a binary complex (**R**–**L**), an energy change due to heat absorbed by or released from interacting molecules will be observed. ITC measures the energy variation in the binding process through heat exchange between a reference and a heat source necessary to maintain the reference and a sample cell at the same temperature during the measurement (Fig. 14) [50, 51].

Biological reactions involving the binding of molecules occur at constant pressure. Under these conditions, the heat (q) released or absorbed from the system is proportional to the enthalpy of the reaction (ΔH^0) at a system temperature (T) and to the number of moles of the resulting complex (n_c), according to the following equation:

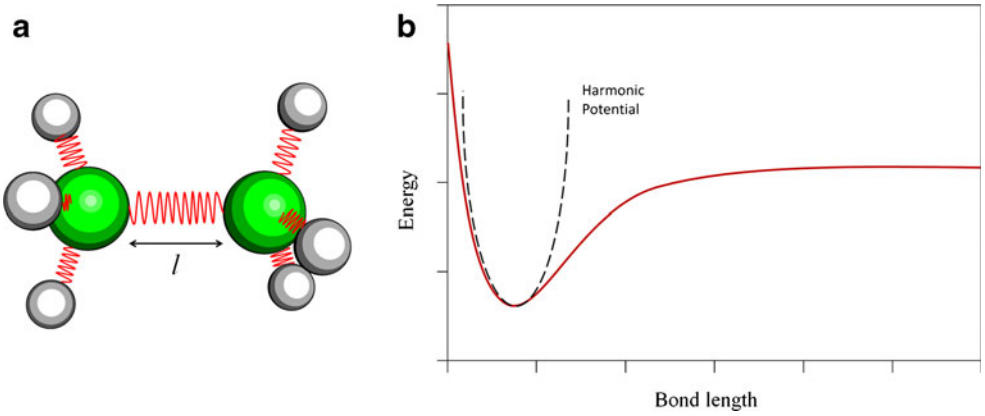

Fig. 11 **a** Spring model used to calculate bond stretching energies for atoms covalently bonded. **b** Harmonic potential (*dashed black curve*) describing energy changes owing to changes in the bond length *l*. Near the natural bond length, the harmonic potential is very similar to the bond potential of the real system (*red continuous curve*; colored online)

$$q = n_c \Delta H^0{}_{(T)} \ . \tag{11}$$

When we express the number n_c of binding complexes in the system as the product of its concentration **[R–L]** by the system volume V, Eq. (11) can be rewritten to the form

$$q = [R\text{–}L] V \Delta H^0{}_{(T)} \ . \tag{12}$$

After the addition of a ligand, the concentrations **[R]**, **[L]**, and **[R–L]** of the species in the system will change as the reaction reaches equilibrium. Since it is not possible to determine the exact concentration of the complex **[R–L]** at a specific instant during the global binding reaction, Eq. (12) would be more useful if expressed with known parameters. Since the receptor is stable under the assay conditions during the ITC binding experiments, the total receptor concentration $\mathbf{[R_{Total}]}$, which is known, will remain constant and represent the sum of the free and bound forms **[R]** and **[R–L]**, respectively, as shown in Eq. (13):

$$[R_{Total}] = [R\text{–}L] + [R]. \tag{13}$$

One can now extract the unbound receptor concentration **[R]** from Eq. (3) and substitute the result on the right-hand side of Eq. (13) to obtain the following equation:

$$[R_{Total}] = [R\text{–}L] + \frac{[R\text{–}L]}{[L]K_d}, \tag{14}$$

rearrangement of which yields the relation

$$[R - L] = [R_{Total}] \left(\frac{[L]}{[L] + K_d} \right). \tag{15}$$

Finally, substitution of (15) into (12) leads to the following equation for q:

$$q = V \Delta H^0{}_{(T)} \ [R_{Total}] \left(\frac{[L]}{[L] + K_d} \right). \tag{16}$$

Equation (16) relates the heat q produced during the binding assay reaction (i. e., measured during the ITC experiment), to the enthalpy $\Delta H^0{}_{(T)}$ and binding constant K_d. The concentration of unbound ligand in solution **[L]** can also be related to the concentrations $\mathbf{[L_{Total}]}$, $\mathbf{[R_{Total}]}$ and parameter K_d. In the expression

$$[L_{Total}] = [R\text{–}L] + [L], \tag{17}$$

we substitute the right-hand side of Eq. (15) for **[R–L]**, to find that

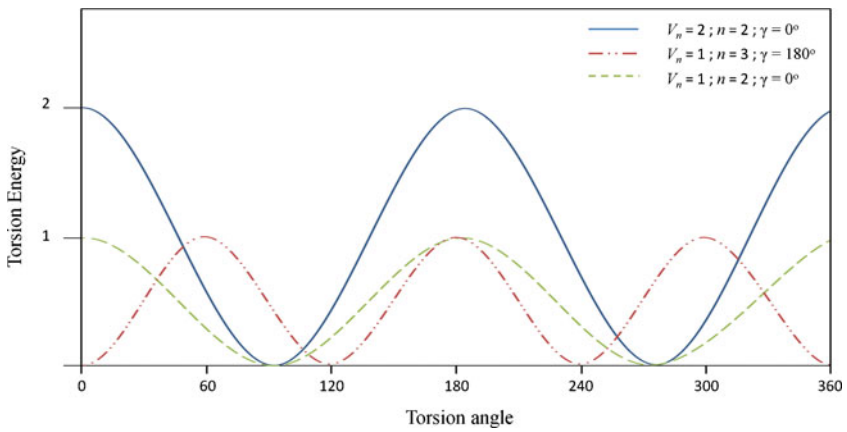

Fig. 12 Torsional energy profiles for dihedrals containing different values of potential barrier (V_n), multiplicity (n), and phase factor (γ) (colored online)

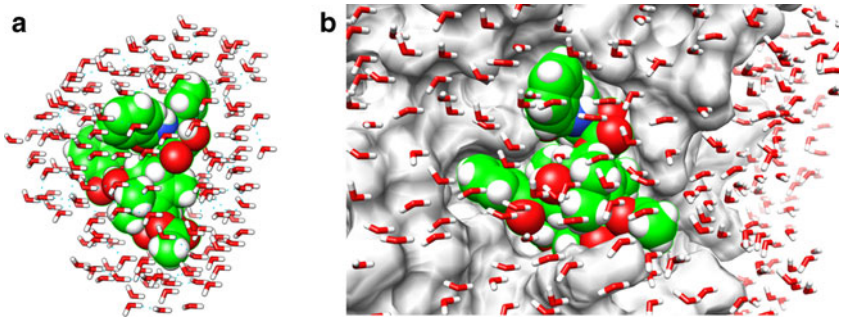

Fig. 13 Solvation of Taxol in solution (**a**) and in its complex to β-tubulin (**b**) (colored online)

$$[L_{Total}] = [R_{Total}]\left(\frac{[L]}{[L]+K_d}\right) + [L] \tag{18}$$

This equation can be rearranged to give the result

$$[L]^2 + [L](K_d + [R_{Total}] - [L_{Total}]) - [L_{Total}]K_d = 0, \tag{19}$$

and finally, Eq. (19) can be solved for **[L]**:

$$[L] = \frac{[L_{Total}] - K_d - [R_{Total}] \pm \sqrt{([R_{Total}] + K_d - [L_{Total}])^2 + 4[L_{Total}]K_d}}{2}. \tag{20}$$

Therefore, the equation for the heat change during an ITC experiment of ligand binding expressed as a function of K_d and $\Delta H^0{}_{(T)}$, as well as of the assay parameters V, $\mathbf{[R_{Total}]}$, and $\mathbf{[L_{Total}]}$, can be obtained by combining Eqs. (16) and (20). Unfortunately, one of the two parameters K_d and $\Delta H^0{}_{(T)}$ can only be directly determined in a single experiment when the other parameter is known. To overcome this problem and determine K_d and $\Delta H^0{}_{(T)}$ in a single assay, ITC experiments are carried out using incremental additions of fixed small amounts of ligand to the solution, through a periodic titration process. This method leads to the observation of heat changes peaks for each ligand injection at a time interval i (Fig. 15). During the initial injections, the amount of ligand injected is much smaller than the number of free receptors and a high number of complexes are formed, resulting in substantial heat changes. After a few injections, the number of free binding sites decreases and the concentration of free (unbound) receptor becomes a limiting factor for the formation of the complexes. The saturation of the binding sites results in a progressive decrease of the ratio between the heat change and the amount of ligand injected. After several injections, there will be no receptors free for binding and heat changes are no longer observed.

The heat change (q_i) produced by the injection of a small amount $\mathbf{[L]}_i$ of ligand in the time interval i corresponds to the area under the ITC peak and can be calculated as the difference between the heat changes of the two succeeding intervals, given by Eq. (16):

$$q_i = V\Delta H^0{}_{(T)}\ [R_{Total}]\left(\frac{[L]_i}{[L]_i + K_d} - \frac{[L]_{i-1}}{[L]_{i-1} + K_d}\right). \tag{21}$$

The resultant curve of the ITC experiment (dashed red line in Fig. 15) can be used to fit Eq. (21) and to determine the values of K_d and $\Delta H^0{}_{(T)}$. Once these values are determined, the free energy of binding $\Delta G_{(T)}$ and the entropy $\Delta S_{(T)}$ involved in this process can be obtained using Eqs. (6) and (4), respectively.

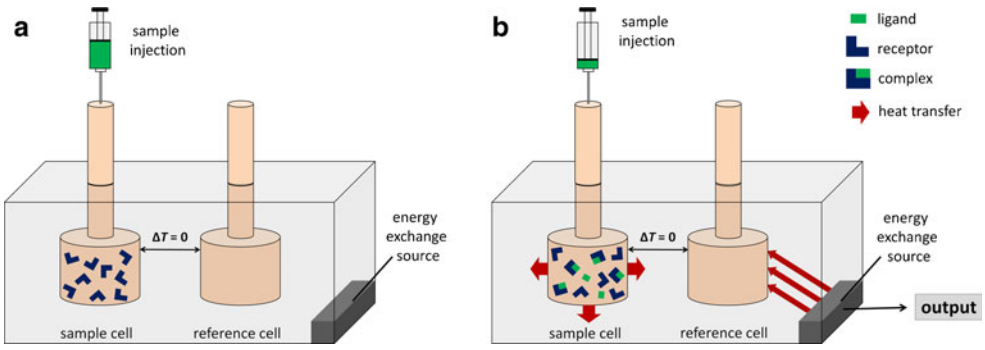

Fig. 14 Schematic illustration of an ITC experiment. **a** Test ligand is injected in a sample cell containing a solution with a known concentration of receptor. Before the sample injection, the temperature difference between the sample and reference cells is zero. **b** The ligand injected binds to the receptor to form a complex. This process can absorb or release energy, resulting in heat exchange with the sample cell that tends to change its temperature. To keep the sample and reference cells at the same temperature, the heat source promotes heat exchange with the reference cell. The heat exchange (either addition or withdrawal of energy from the source) can be measured to quantify the energy associated with the receptor–ligand complex formation (colored online)

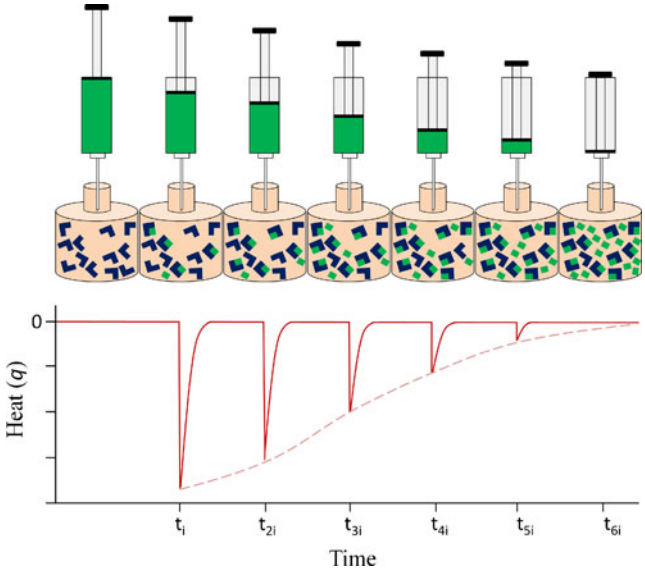

Fig. 15 Typical output of an ITC experiment. Peaks of heat change are observed after each injection of a small quantity of ligand over time in a solution containing the target receptor (colored online)

The use of ITC to evaluate the activity of compounds selected by *structure-based virtual screening* is now widespread and represents a robust method to study binding affinities.

Several bioactive compounds have been evaluated and validated in drug discovery projects with a variety of molecular targets [52, 53]. The combination of ITC with molecular modeling is an elegant approach that reveals important molecular mechanisms related to receptor–ligand complex formation [51–54].

8 Concluding Remarks

Recent scientific and technological progress has brought about a revolution in drug discovery, presenting new opportunities for scientists and students at many different stages of their research projects or careers. *Structure-* and *ligand-based drug design* approaches have been successfully applied in hit identification and lead optimization across a range of key therapeutic targets, playing a crucial role in modern medicinal chemistry. In this scenario, the understanding of protein–ligand interactions is essential for the design of ligands with improved affinity, selectivity and biological potency. In this paper we presented the basic physical principles applied to medicinal chemistry and drug design to help scientists expand their creative role and contribute to bringing the next generation of new drugs to the market. Taxol is an important example of anticancer compound used in chemotherapy, which interferes with microtubule dynamics through its specific binding to the β-subunit of tubulin (ESM 2 and 3). We have also shown that the predicted biological parameters (e.g., biological activity, energy, and binding equilibrium) can be validated and quantified by experimental studies. Without a doubt, deeper understanding of the molecular features related to drug binding is of great importance to drive the scientific spirit of experienced researchers, and to strongly encourage creativity, imagination and invention as an extraordinary opportunity for students and young scientists. This is an open door for innovation, and we believe that physics will continue to play an increasingly important role in future drug discovery.

Acknowledgments We thank the São Carlos Institute of Physics (*Instituto de Física de São Carlos*) for providing an interesting and unique interdisciplinary research environment in the area of medicinal chemistry and drug design.

References

1. WHO, World Health Statistics Report. (World Health Organization, 2012), http://www.who.int/gho/publications/en/. Accessed 8 May 2013
2. T.L. Moda, L.G. Torres, A.E. Carrara, A.D. Andricopulo, Bioinformatics **24**, 2270 (2008)
3. P. Kirkpatrick, Nat. Rev. Drug. Discov. **8**, 196 (2009)
4. S.M. Paul, D.S. Mytelka, C.T. Dunwiddie, C.C. Persinger, B.H. Munos, S.R. Lindborg, A.L. Schacht, Nat. Rev. Drug Discov. **9**, 203 (2010)
5. Y. Zhao, E.B. Butler, M. Tan, Cell Death Dis. **4**, e532 (2013)
6. R.N. Santos, R.V. Guido, G. Oliva, L.C. Dias, A.D. Andricopulo, Med. Chem. **7**, 155 (2011)
7. L.G. Ferreira, R.N. Santos, A.D. Andricopulo, J. Braz. Chem. Soc. **24**, 201 (2013)
8. M. Baker, Nat. Rev. Drug Discov. **12**, 5 (2013)
9. R.V.C. Guido, G. Oliva, A.D. Andricopulo, Pure Appl. Chem. **84**, 1857 (2012)
10. C. Harrison, Nat. Rev. Drug Discov. **12**, 101 (2013)
11. T.I. Oprea, R. Mannhold, H. Kubinyi, G. Folkers, *Chemoinformatics in drug discovery*, 1st edn. (Wiley, Weinheim, 2005), pp. 59–101
12. B. Alberts, A. Johnson, J. Lewis, M. Raff, K. Roberts, P. Walter, *Molecular biology of the cell*, 5th edn. (Garland Science, New York, 2008), p. 63
13. M. Rask-Andersen, M.S. Almén, H.B. Schiöth, Nat. Rev. Drug Discov. **10**, 579 (2011)
14. D.L. Nelson, M.M. Cox, *Lehninger principles of biochemistry*, 5th edn. (W.H. Freeman, New York, 2009), pp. 71–85
15. F. Chiti, C.M. Dobson, Annu. Rev. Biochem. **75**, 333 (2006)
16. A.M. Bode, Z. Dong, Nat. Rev. Cancer **9**, 508 (2009)
17. P.S. Steeg, Nat Med. **12**, 895 (2006)
18. Cancer Facts & Figures 2013. (American Cancer Society, 2013), http://www.cancer.org/research/cancerfactsfigures/cancerfactsfigures/cancer-facts-figures-2013. Accessed 11 May 2013
19. P.B. Schiff, J. Fant, S.B. Horwitz, Nature **277**, 665 (1979)
20. J.R. Jackson, D.R. Patrick, M.M. Dar, P.S. Huang, Nat. Rev. Cancer **7**, 107 (2007)
21. M.A. Jordan, L. Wilson, Nat. Rev. Cancer **4**, 253 (2004)
22. A.L. Risinger, F.J. Giles, S.L. Mooberry, Cancer Treat. Rev. **35**, 255 (2009)
23. A.E. Prota, K. Bargsten, D. Zurwerra, J.J. Field, J.F. Díaz, K.H. Altmann, M.O. Steinmetz, Science **339**, 587 (2013)
24. D. Mastropaolo, A. Camerman, Y. Luo, G.D. Brayer, N. Camerman, Proc. Natl. Acad. Sci. USA **92**, 6920 (1995)
25. J.J. Field, J.F. Díaz, J.H. Miller, Chem. Biol. **20**, 301 (2013)

26. D.B. Kitchen, H. Decornez, J.R. Furr, J. Bajorath, Nat. Rev. Drug Discov. **3**, 935 (2004)
27. X.Y. Meng, H.X. Zhang, M. Mezei, M. Cui, Curr. Comput. Aided Drug Des. **7**, 146 (2011)
28. M. Lapelosa, E. Gallicchio, R.M. Levy, J. Chem. Theory Comput. **8**, 47 (2012)
29. R. Macarron, M.N. Banks, D. Bojanic, D.J. Burns, D.A. Cirovic, T. Garyantes, D.V. Green, R.P. Hertzberg, W.P. Janzen, J.W. Paslay, U. Schopfer, G.S. Sittampalam, Nat. Rev. Drug Discov. **10**, 188 (2011)
30. M. Valli, R.N. dos Santos, L.D. Figueira, C.H. Nakajima, I. Castro-Gamboa, A.D. Andricopulo, V.S. Bolzani, J. Nat. Prod. **76**, 439 (2013)
31. J.J. Irwin, T. Sterling, M.M. Mysinger, E.S. Bolstad, R.G. Coleman, J. Chem. Inf. Model. **52**, 1757 (2012)
32. A.R. Leach, *Molecular modelling: principles and applications*, 2nd edn. (Prentice-Hall, New Jersey, 2001), pp. 165–247
33. F.C. Bernstein, T.F. Koetzle, G.J. Williams, E.E. Meyer Jr., M.D. Brice, J.R. Rodgers, O. Kennard, T. Shimanouchi, M. Tasumi, J. Mol. Biol. **112**, 535 (1977)
34. M. Rarey, B. Kramer, T. Lengauer, G. Klebe, J. Mol. Biol. **261**, 470 (1996)
35. I. Halperin, B. Ma, H. Wolfson, R. Nussinov, Proteins **47**, 409 (2002)
36. A.R. Leach, V.J. Gillet, *An introduction to chemoinformatics*, 1st edn. (Springer, Dordrecht, 2007), pp. 159–181
37. E.S. Istvan, J. Deisenhofer, Science **292**, 1160 (2001)
38. M.M.A. Ajay, J. Med. Chem. **38**, 4953 (1995)
39. R.A. Copeland, *Evaluation of enzyme inhibitors in drug discovery: a guide for medicinal chemists and pharmacologists*, 2nd edn. (Wiley, New Jersey, 2013), pp. 1–54
40. J. De Heer, *Phenomenological thermodynamics with applications to chemistry*, 4th edn. (W. H. Freeman, New York, 1990), pp. 5–60
41. D.A. Pearlman, P.A. Kollman, J. Chem. Phys. **91**, 7831 (1989)
42. A. Hinchliffe, *Molecular modelling for beginners*, 2nd edn. (Wiley, London, 2008), pp. 49–63
43. K.M. Merz, D. Ringe, C.H. Reynolds, *Drug design: structure- and ligand-based approaches*, 1st edn. (Cambridge University Press, Cambridge, 2010), pp. 61–119
44. M. Born, J.R. Oppenheimer, Ann. Phys. **389**, 457 (1927)
45. P. Graham, *Introduction to medicinal chemistry*, 5th edn. (Oxford University Press, New York, 2013), pp. 1–28
46. C. Bissantz, B. Kuhn, M. Stahl, J. Med. Chem. **53**, 5061 (2010)
47. C.M. Breneman, K.B. Wiberg, J. Comput. Chem. **11**, 361 (1990)
48. M. Rigby, E.B. Smith, W.A. Wakeham, G.C. Maitland, *An introduction to intermolecular forces* (Clarendon Press, Oxford, 1986), pp. 3–80
49. J. Gasteiger, M. Marsili, Tetrahedron **36**, 3219 (1980)
50. K.E. van Holde, C. Johnson, P.S. Ho, *Principles of physical biochemistry*, 2nd edn. (Prentice-Hall, New Jersey, 2006), pp. 99–103
51. M.W. Freyer, E.A. Lewis, Methods Cell. Biol. **84**, 79 (2008)
52. P.O. Tsvetkov, A.A. Makarov, S. Malesinski, V. Peyrot, F. Devred, Biochimie **94**, 916 (2012)
53. B.M. Baker, K.P. Murphy, Biophys. J. **71**, 2049 (1996)
54. E. Freire, Drug Discov. Today Technol. **1**, 295 (2004)